

JP6J.6 INFLUENCE OF SURFACE CHARACTERISTICS ON SENSIBLE AND LATENT HEAT FLUXES AND BOUNDARY LAYER MESOSCALE CIRCULATIONS

Margaret A. LeMone,* Fei Chen, Joseph G. Alfieri, and Mukul Tewari
National Center for Atmospheric Research, Boulder Colorado

Bart Geerts and Qun Miao
Department of Meteorology, University of Wyoming

Richard Coulter
Argonne National Laboratory, Argonne, Illinois

Robert Grossman
Colorado Research Associates, Boulder Colorado

1. INTRODUCTION

Numerous modeling studies by Anthes (1984), Segal et al. (1988), Pielke et al. (1991), and others have used idealized or specific case studies to how a heterogeneous land surface could generate ~10-100 km mesoscale circulations and then either initiate or reinforce precipitating convection. Chen et al. (1997) showed that accounting for these surface processes improved quantitative precipitation forecasts in the Eta model as much as doubling the horizontal resolution. Here, we use IHOP_2002 and CASES-97 data from the same location in SE Kansas to illustrate the effects of the land surface on fluxes, and to discuss the formation of mesoscale circulations on 30 May 2002.

2. DATA COLLECTION AND ANALYSIS

Measurement of sensible heat flux H and latent heat flux LE are based on repeated (4-10) flight legs by the University of Wyoming King-Air gust-probe aircraft, taken over the IHOP_2002 Eastern Flight Track (Figure 1). The flight level was 40 m above ground level (agl) during CASES-97, and 65-70 m agl during IHOP_2002. The data were collected over ~4 h, at 1430-1830 UTC for CASES-97, and at 1630-2030 UTC for IHOP_2002; local solar noon ~1830 UTC. The data were detrended before computing the fluxes, averaged into 1-km blocks, interpolated to common points, filtered using a 4-point running mean filter, and then averaged to form a grand-average leg for each day. The repeated legs and

the 4-km running averages provide reasonably robust flux estimates and largely eliminate the flux-concentration effects of large eddies, which can mask the effects of the surface (LeMone et al. 2003). During each mission 1-3 other heights were sampled as well, affording the opportunity to obtain flux and divergence profiles, and to extrapolate the low-level fluxes to the surface. For IHOP_2002, the aircraft and surface fluxes were in good agreement, but the aircraft H fluxes in CASES-97 were probably too low.

Boundary layer depth was obtained from aircraft leg-end soundings, the Wyoming Cloud Radar (Pazmany et al. 1994, Miao et al. 2005), and the Argonne Boundary Layer Experiments (ABLE) facility wind profilers at Beaumont and Oxford (LeMone et al. 2000, Miller et al. 2005), which lie near the west (Oxford) and east (Beaumont) ends of the Eastern Track.

Surface information along the flight track is from a forward-looking video, Normalized Differential Vegetation Index (NDVI) from an Exotech Radiometer, and radiometric surface temperature T_s from a Heiman KT-19.85 radiometer.

3. RESULTS

3.1 Fluxes

Figure 2 illustrates the relationship between H and LE to T_s and NDVI on 22 June 2002, when the wind was out of the south at 9.4 m s^{-1} . In the figure, the H maximum (LE minimum) corresponds to high T_s and low NDVI, while the H minimum (LE maximum) corresponds to low T_s and high NDVI. The NDVI minimum and T_s maximum correspond to a large area of already-harvested winter wheat, grown in the lowlands south of Timber Creek

*Corresponding author address: Margaret A. LeMone, National Center for Atmospheric Research, P.O. Box 3000, Boulder, CO 80307; e-mail: lemone@ucar.edu

Lake; while the broad T_s minimum and NDVI maximum reflects the grasslands (green) to the east, which in turn tend to be associated with higher terrain and shallow soil. From Figure 1, the grassland-east and winter-wheat west pattern continues southward. The secondary peak reflects the area of upstream winter wheat around -96.7° . The H pattern on 30 May 2002 (wind $159^\circ/3.9 \text{ m s}^{-1}$) is similar to 22 June. At this longitude, the track crosses a ridge, which should enhance sensible heat fluxes because of the associated shallow soils and loss of surface and subsurface moisture due to surface and subsurface flow. On 17 June 2002 (wind $201^\circ/7.7 \text{ m s}^{-1}$) and 20 June 2002 ($162^\circ/5.3 \text{ m s}^{-1}$), the H maximum at this longitude is as large as that at -96.9° . During CASES-97, when the winter wheat is green and the grasses dormant, the H, LE, and T_s extrema reverse (Figure 3).

3.2 Temperature Patterns

CASES-97 and IHOP_2002 have their own characteristic potential-temperature Θ patterns (Figure 4). For the two CASES-97 days, there is a Θ maximum near the center of the track; while Θ increases westward on all four IHOP_2002 days, with the strongest temperature contrast on 30 May. In IHOP_2002, the patterns are clearly related to the vegetation distribution upstream (south) of the flight track, with more dormant to harvested winter wheat to the west (higher H) and more grasses (low H) to the east (Fig. 1). This pattern continues south to the Oklahoma-Kansas border ($\sim 100 \text{ km}$); to the south, the belt of winter wheat extends southwestward through Oklahoma. On 30 May, the effects of vegetation on upstream warming are reinforced – or even dominated – by the effects of an area of high soil moisture to the southeast. Indeed, the cooler air along the eastern half of the track maintains the same mixing ratio through the flight pattern, while the warmer air along the western half of the track becomes drier through the flight as the boundary layer grows (Fig. 4). The Wyoming Cloud radar, the ABLER radar wind profilers, and the aircraft soundings consistently indicate the BL is deeper at the west end of the flight track on all the IHOP_2002 days, but deeper at the east end of the track in CASES-97 (Table 1).

3.3 Mesoscale Circulations

Our analysis of the 4 IHOP_2002 days is consistent with the conventional wisdom that mesoscale circulations are favored on days with

light winds. In the simplest case, we expect mesoscale circulations if (a) the synoptic forcing is weak (consistent with light winds), and (b) if there is a mesoscale temperature gradient of sufficient magnitude and horizontal scale for air passing through to have a dynamic response. To obtain the time constant $\Delta t_{\Delta\Theta_v}$ for developing a horizontal virtual-temperature difference through the BL, $\Delta\langle\Theta_v\rangle$, we assume (a) that the buoyancy flux over the upstream winter wheat is 20% higher than that over the grasslands, (b) that the boundary layer height is the same over both regions (consistent with a strong inversion), and (c) that the flux $\overline{w\theta_{v,zi}}$ at the top of the boundary layer z_i is related to the surface buoyancy flux $\overline{w\theta_{v,0}}$ via $\overline{w\theta_{v,zi}} = -0.2\overline{w\theta_{v,0}}$:

$$\Delta t_{\Delta\Theta_v} \sim \frac{\Delta\langle\Theta_v\rangle z_i}{0.24\overline{w\theta_{v,0}}} \quad (1)$$

The horizontal scale $D_{\Delta\Theta}$ required to develop $\Delta\langle\Theta_v\rangle$ can be found by multiplying (1) by the wind speed S . For $z_i = 1000 \text{ m}$, $\overline{w\theta_{v,0}} = 0.1 \text{ K m s}^{-1}$, $\Delta\langle\Theta_v\rangle = 0.5 \text{ K}$, and $S = 5 \text{ m s}^{-1}$, $\Delta t_{\Delta\Theta_v} = 5.8 \text{ h}$ and $D_{\Delta\Theta} = 104 \text{ km}$. Although both $\overline{w\theta_{v,0}}$ and z_i change with time, their ratio varies less in the morning hours preceding and including the IHOP_2002 measurements, so (1) still applies in a crude sense. To obtain the characteristic time for response to $\Delta\langle\Theta_v\rangle$, we rearrange the circulation equation for a two-dimensional temperature field, and apply the hydrostatic equation, to obtain:

$$\Delta t_{\Delta u} \sim 2\Delta u \left[\frac{4.9z_i}{\langle\Theta_v\rangle} \frac{\Delta\langle\Theta_v\rangle}{s} \right]^{-1} \quad (2)$$

For the same conditions, $\langle\Theta_v\rangle = 300 \text{ K}$, flight-track length $s = 46 \text{ km}$, and $\Delta u = 1 \text{ m s}^{-1}$, $\Delta t_{\Delta u} = 3.1 \text{ h}$ and $D_{\Delta u} = 56 \text{ km}$. A small ratio $\Delta t_{\Delta u} / \Delta t_{\Delta\Theta_v}$ or $D_{\Delta u} / D_{\Delta\Theta}$ means that there is time for mesoscale circulations to develop.

The response of an air parcel crossing an infinite two-dimensional temperature-change zone of finite

width increases with the time crossing the zone. This response can be obtained from the circulation equation via:

$$\frac{\partial u_s}{\partial s} \sim \frac{R}{2u_s} \frac{\partial \langle \Delta \Theta_v \rangle}{\partial s} \ln \frac{p_o}{p_s} \quad (3)$$

Table 2 summarizes the parameters associated with development of mesoscale circulations. From Table 2, 30 May not only has ample time to develop mesoscale circulations but the small along-track wind allows a strong response.

With a rapid dynamic response compared to the setup time (or distance) for $\Delta \langle \Theta_v \rangle$, the resulting circulation will destroy the temperature gradient unless vertical flux divergence can just cancel the horizontal advection associated with the circulation. If we follow a cold-to-warm trajectory and assume a 20% jump in $\overline{w\theta_{v,0}}$ along the trajectory, we can use (1) to describe the time needed to increase $\langle \Theta_v \rangle$ by $\Delta \langle \Theta_v \rangle$. For $z_i = 1000$ m and $\overline{w\theta_{v,0}} = 0.1$ K m s⁻¹, the associated distance is $42 \Delta \langle \Theta_v \rangle$ km. *Under these assumptions*, steady-state mesoscale circulations would have to be 42 km wide to maintain $\Delta \langle \Theta_v \rangle = 1$ K. However, it should be noted that numerous large-eddy simulations of boundary layers over idealized alternating moist and dry patches have produced mesoscale circulations of smaller scale in an average sense (see Patton et al. 2005 and references therein), and Grossman et al. (2005) show evidence of a 10-km circulation for a grand average leg along the Eastern Track for CASES-97.

Figure 5 shows the evolution of BL temperature and vertical velocity field on 30 May from a WRF model simulation (<http://www.wrf-model.org>). Note the development of an area of positive vertical velocity (W) centered over the temperature maximum that lies just to the west of the ABLE array (triangle), with a minimum to the south and east. The WRF model was initialized using the EDAS soil-moisture field, which is available from NCEP at 40-km resolution. Two nested domains were used, centered on the IHOP_2002 domain: an outer 3480 x 3000-km domain with 12-km

spacing, and an inner 1800 x 1550-km domain with 4-im spacing.

Both the spatial scale and magnitude of the temperature change are significantly larger than appears in Table 2 because of the large scale of the soil moisture and vegetation patterns that control the fluxes and hence BL warming and moistening. The temperature minima and maxima correspond well to areas of high and low soil moisture. Fortuitously, the high soil moisture to the southeast corresponds to grasses, while the dry soil moisture to the west of the ABLE domain (triangle) corresponds to harvested winter wheat. As noted previously, the combined effects of vegetation and soil moisture on 30 May set up the strongest temperature contrast of the four days.

Both the radar wind profiler vertical velocities and the along-track convergence are consistent with but not definitive evidence for mesoscale circulations on 30 May. The radar wind profiler W (not shown) remains small on 30 May, while on the other days the W-profiles reflect the strong subsidence associated with fair weather. The aircraft shows along-track convergence in the lower BL, and along-track divergence in the upper BL on 30 May, with divergence on two days and convergences in the noise on the third.

4. CONCLUSIONS

Flux measurements along the same flight track in southeast Kansas along, taken over two phases in the local vegetation growing cycles from 29 April to 10 May (CASES-97, winter wheat green, grass beginning to green up) and from 30 May to 22 June (IHOP_2002, winter wheat dormant-to-harvested, grass green), show clearly the association of H and LE to the horizontal distribution of vegetation. In both experiments, H maxima (LE minima) occur over/just downstream of dormant vegetation, while H minima (and LE maxima) occur over/just downstream of green vegetation. The upstream vegetation distribution leads to a repeatable warm-west to cool-east pattern in potential temperature along the flight track. On 30 May, soil moisture distribution reinforces the upstream vegetation to create the strongest contrast of the four days. The light winds and the strong virtual temperature gradients on this day led to the development of ~100-km circulations.

References

- Anthes, R.A., 1984: Enhancement in convective precipitation by mesoscale variations in vegetative covering in semiarid regions. *J. Clim. Appl. Meteor.*, **23**, 541-554.
- Chen, F., Z. Janjic, and K. Mitchell, 1997: Impact of atmospheric surface layer parameterization in the new land-surface scheme of the NCEP mesoscale Eta numerical model. *Bound.-Layer Meteor.*, **185**, 391-421.
- Grossman, R.L., D. Yates, M.A. LeMone, M.L. Wesely, and J. Song, 2005: Observed effects of horizontal radiative surface temperature variations in the atmosphere over a Midwest watershed during CASES-97. *J. Geophys. Res.*, **110**, D06117, doi:10.1029/2004JD004542.
- LeMone, M.A., and Coauthors, 2000: Land-atmosphere interaction research and opportunities in the Walnut River watershed in southeast Kansas: CASES and ABLE. *Bull. Amer. Meteor. Soc.*, **81**, 757-779.
- LeMone, M.A., and Coauthors, 2002: Late-morning warming and moistening of the convective boundary layer over the Walnut River watershed. *Bound.-Layer Meteor.* **104**, 1-52. *J. Hydromet.*, **4**, 179-195.
- LeMone, M.A., R.L. Grossman, F. Chen, K. Ikeda, and D. Yates, 2003: Choosing the averaging interval for comparison of observed and modeled fluxes along aircraft transects of a heterogeneous surface. *J. Hydrometeor.*, **4**, 179-195.
- Miao, Q., B. Geerts, and M.A. LeMone, 2005: Vertical velocity and buoyancy characteristics of coherent echo plumes in the convective boundary layer, determined by a profiling airborne radar.
- Miller, N.L., and Coauthors, 2005: The DOE water cycle pilot study. *Bull. Amer. Meteor. Soc.*, **86**, 359-374.
- Patton, E.G., P.P. Sullivan, and C.-H. Moeng, 2005: The influence of idealized heterogeneity on wet and dry planetary boundary layers coupled to the land surface. *J. Atmos. Sci.*, **62**, 2078-2097.
- Pazmany, A., R. McIntosh, R. Kelly, and G. Valli, 1994: An airborne 94-GHz dual-polarized radar for cloud studies. *IEEE Trans. Geosci. And Remote Sensing*, **32**, 731-739.
- Pielke, R.A., G. Dalu, J. Snook, T. Lee, T. Kittell, 1991: Nonlinear influence of mesoscale land use on weather and climate. *J. Climate*, **4**, 1053-1069.
- Segal, M., R. Avissar, M. McCumber, and R. Pielke, 1988: Evaluation of vegetation effects on the generation and modification of mesoscale circulations. *J. Atmos. Sci.*, **45**, 2268-2292.

Table 1. East-west differences in BL height (m) along the Eastern Track. E = east end of the track; W=west end of the track.

| Date | ABLE W | ABLE E | $z_i(W) - z_i(E)$ King Air Sdgs | $z_i(W) - z_i(E)$ WCR |
|-------------|---------------|---------------|------------------------------------|--------------------------|
| 29 April 97 | 1050 (at OXF) | 1200 (at BEA) | | |
| 10 May 97 | 1300 (at OXF) | 1500 (at BEA) | | |
| 30 May 02 | 927 | 838 | 50 | 100 |
| 17 June 02 | 1336 | 1143 | 150 | 75 |
| 20 June 02 | ~1300 (est)* | ~1200 (est) | 100 | 100 |
| 22 June 02 | 1304 | 1212 | 100 | M |

*From soundings.

Table 2: Criteria for development of mesoscale circulations along the flight track for IHOP_2002

| Date | $\Delta\Theta_{v=}$ $\Theta_v(W) - \Theta_v(E)$ at 70 m (avg) | $\Delta\Theta_v$ rest of BL (avg) | 70-m Wind (avg) | u_s at 70 m (avg) | $\frac{\partial u_s}{\partial s}$ (3) | $\frac{\Delta t_{\Delta\Theta_v}}{\Delta t_{\Delta u}}$ for observed $\langle \Theta_v \rangle$ and $\Delta u_s = -1$ |
|---------|--|---|-----------------------|---------------------------|--|--|
| | (K) | (K) | $m s^{-1}$ | $m s^{-1}$ | $(10^{-4} s^{-1})$ | |
| 30 May | 0.7 | 0.6 | 3.9 | 0.3 | 6.4 | 0.2 |
| 17 June | 0.4 | 0.4 | 7.7 | 5.5 | 0.35 | 0.3 |
| 20 June | 0.3 | 0.3 | 5.3 | 0.69 | 1.97 | 0.5 |
| 22 June | 0.2 | 0.2 | 9.4 | 3.8 | 0.22 | 1.2 |

"Cool": value at 1830 UTC calculated so that the average of the "warm" and "cool" values equal the leg averages.

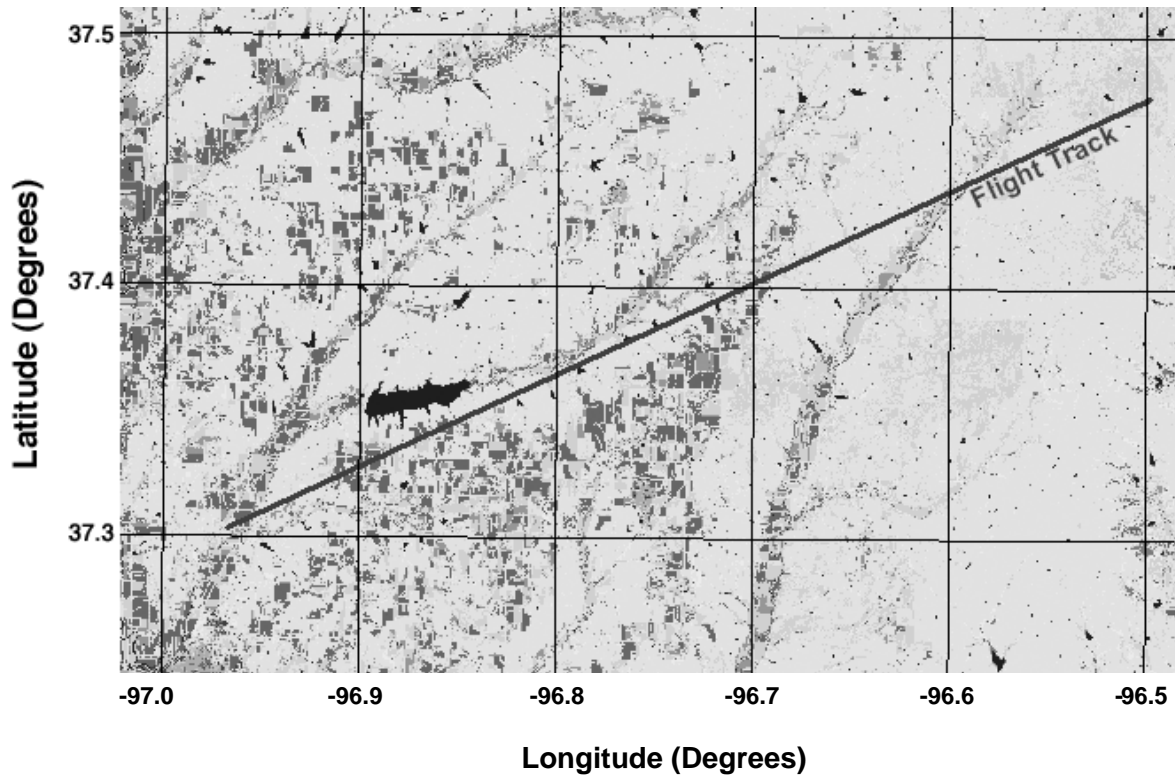


Figure 1. IHOP_2002 Eastern Track, superimposed on land use based on NLCD 1992 (<http://landcover.usgs.gov>). Light gray: grasslands; medium and dark gray: crops (mostly winter wheat; some trees along streams), black: open water. The large lake is Timber Creek Lake.

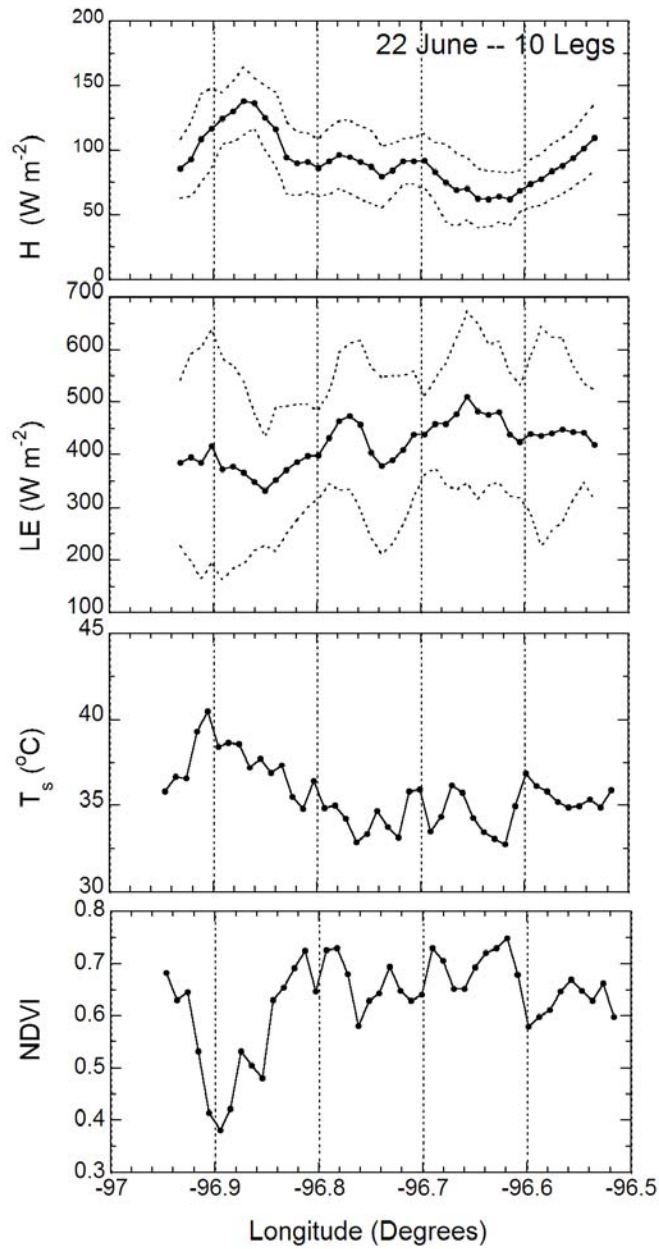


Figure 2. For 22 June 2002, 4-km running-mean grand-average H and LE (solid) along the track in Fig. 1, with standard deviations (dashed), between 1708 and 2104 UTC (solar noon ~ 1830 UTC). Lower frames show 1-km grand average T_s and NDVI.

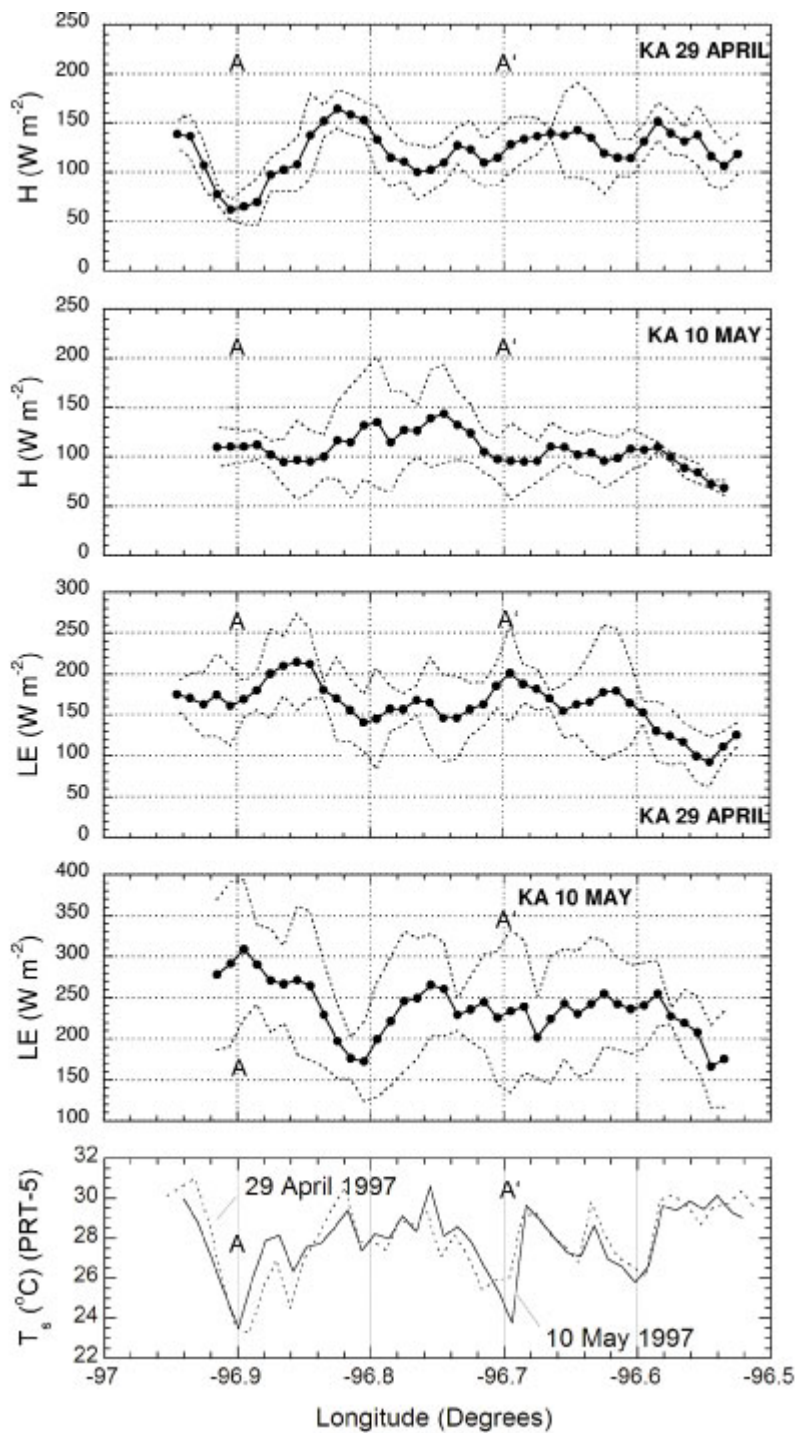


Figure 3. As in Figure 2, but for 29 April and 10 May 1997, and there is no NDVI.

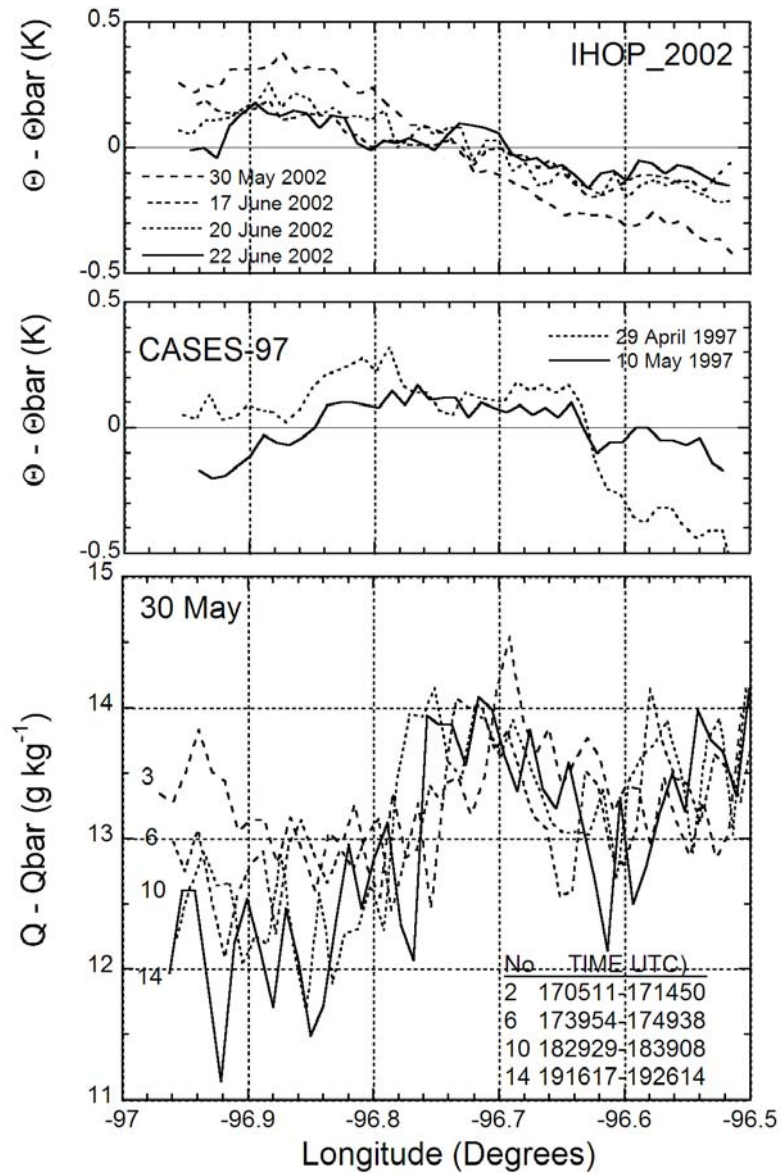


Figure 4. (top) grand-average ~1-km potential temperature at the lowest flight level for CASES-97 (30-40 m agl) and IHOP_2002 (70 m agl); (bottom) grand-average ~1 km mixing ratio Q for 4 flight legs at 70 m agl. Note that the elevation beneath the western end of the track is 150 m lower than the eastern end, so the actual temperature contrast would be even stronger for IHOP_2002.

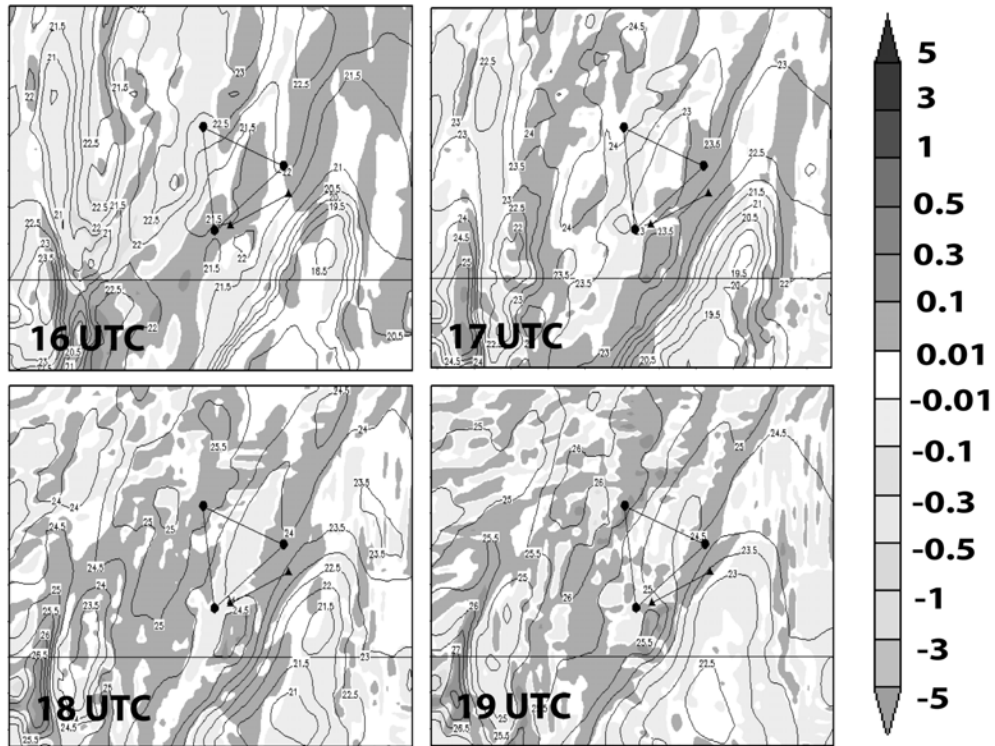


Figure 5: For 1600-1900 UTC 30 May, vertical velocity W (m s^{-1} shading) at Level 5 (~ 500 m agl, mid-upper BL) and temperature ($^{\circ}\text{C}$, contours) at Level 3 (~ 300 m agl low-mid BL). The triangle connects the three ABL wind profilers. Oxford (OXF) is near the west end of the flight track, and Beaumont near the east end. Length of flight track: ~ 46 km; length of sides of triangle ~ 60 km.